How to cite: *Angew. Chem. Int. Ed.* **2025**, e202504835
doi.org/10.1002/anie.202504835

CO_2 Reduction | Hot Paper

Efficient Bicarbonate Electrolysis to Formate Enabled via Ionomer Surface Modification in Cation Exchange Membrane Electrolyzers

*Kewen Xing, Mengjing Wang, Binbin Pan, Chenglin Liang, and Yanguang Li**

Abstract: Electrochemical CO_2 reduction (CO_2RR) is a promising method for converting CO_2 into valuable chemicals, with formate being a particularly viable product. However, current gas-fed CO_2RR systems rely on highly pure CO_2 feed gases and are incompatible with point-source CO_2 emissions without prior capture and concentration. Bicarbonate electrolysis offers a potential solution by bridging the gap between CO_2 emissions and utilization. However, existing electrolyzer configurations, especially those using bipolar membranes (BPM), require high working voltages and suffer from poor energy efficiency. Here, we present a cation exchange membrane (CEM)-based membrane electrode assembly (MEA) incorporating a surface-modified bismuth cathode catalyst. The success of this approach is attributed to two key factors: the use of the positively charged ionomer PiperION for surface modification, which creates a favorable cathode microenvironment; the single CEM that enhances proton flux from the anode to the cathode while reducing ionic impedance. The CEM-based MEA demonstrates a formate faradaic efficiency of up to 80%, with a significant 1.5 V reduction in operating voltage compared to BPM-based MEAs at 300 mA cm^{-2}. Additionally, the CEM-based MEA exhibits excellent tolerance to O_2 impurities and maintains high performance even with simulated flue gas, making it suitable for direct CO_2 utilization from point sources.

Electrochemical CO_2 reduction reaction (CO_2RR) offers a promising solution for converting CO_2 into value-added chemicals.[1,2] Among the possible reduction products, formic acid or formate has garnered particular attention due to its high economic viability.[2–4] Current research has primarily focused on gas-fed CO_2RR systems such as flow cells and membrane electrode assemblies (MEAs), which deliver CO_2 directly to the catalyst through gas diffusion electrodes (GDEs).[5–7] Despite impressive current densities achieved (up to >1 A cm^{-2}), several challenges remain in these systems (Figure 1a).[8–12] One major issue is the undesirable formation of (bi)carbonate, which crosses the commonly used anion exchange membrane to the anode, compromising CO_2 conversion efficiency and introducing a high energy penalty for CO_2 recovery.[8–10] (Bi)carbonate salt can also precipitate in the GDE pores, leading to premature device failure. Moreover, these gas-fed electrolyzers rely on highly pure CO_2 feed gases, and their performance significantly deteriorates with even trace amounts of impurities (e.g., O_2).[11,12] This makes it impractical to directly convert flue gases—the primary source of CO_2 emission—using gas-fed systems. To address point-source CO_2 emissions, CO_2 capture and concentration steps are currently essential prior to conversion.[13] For instance, CO_2 can be captured and separated from flue gases through chemical adsorption using amines or alkali bases, forming carbamates or (bi)carbonates. A subsequent thermal or pH swing can reverse the reaction, releasing CO_2 in a pure form.[13,14] However, this CO_2 capture and concentration process complicates the overall system and consumes additional energy. It is estimated that the energy required to capture CO_2 from flue gases using benchmark aqueous monoethanolamine is 181 kJ per mole of CO_2,[15] which is about half of the theoretical energy required to electrochemically convert CO_2 to formic acid (356 kJ per mole of CO_2).

To minimize the energy costs associated with CO_2 capture and concentration, direct electrolysis of chemically adsorbed CO_2 derivatives (i.e., carbamates or (bi)carbonates) would be highly desirable though challenging.[16–19] Studies have shown that these compounds cannot be electrochemically reduced under ambient conditions. To utilize them as carbon sources, the electrolyzer would need to be heated to decompose them back to CO_2, or the electrolyte would need to be acidified to release CO_2.[16,20–23] For instance, Berlinguette and colleagues first introduced a bipolar membrane (BPM)-based flow cell that leveraged the proton flux from water dissociation at the BPM.[21] The protons diffuse to the cathode, and react with (bi)carbonates to generate a localized high concentration of CO_2, which then participates in CO_2RR (Figure 1b). Despite its potential for (bi)carbonate electrolysis, BPM-based systems demand large working voltages (often >4 V at 100 mA cm^{-2}) due to the substantial water dissociation overpotential of the BPM.[24,25] This, in turn, limits the energy efficiency of the system and negates the original motivation for direct (bi)carbonate electrolysis.

[*] K. Xing, M. Wang, Dr. B. Pan, C. Liang, Prof. Y. Li
Institute of Functional Nano & Soft Materials (FUNSOM), Soochow University, Suzhou 215123, China
E-mail: yanguang@suda.edu.cn

K. Xing, M. Wang, Dr. B. Pan, C. Liang, Prof. Y. Li
Jiangsu Key Laboratory for Advanced Negative Carbon Technologies, Soochow University, Suzhou 215123, China

Additional supporting information can be found online in the Supporting Information section

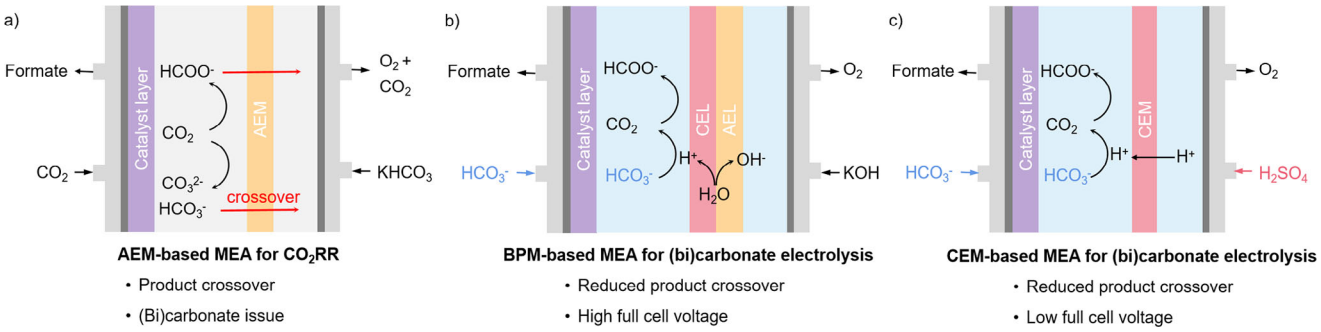

Figure 1. Schematic showing the different configurations of a) gas-fed AEM-based MEA for CO_2RR, b) BPM-based MEA for (bi)carbonate electrolysis, and c) proposed CEM-based MEA for bicarbonate electrolysis.

In this study, we propose that cation exchange membrane (CEM)-based MEAs, operating with an acidic anolyte, can similarly provide the necessary proton flux to react with (bi)carbonates at the cathode, while the single membrane configuration significantly reduces the overall working voltage (Figure 1c). To achieve optimal performance for bicarbonate electrolysis, a bismuth catalyst is selected, and its surface is functionalized with a positively charged ionomer to mitigate local proton buildup. When fed with a $KHCO_3$ aqueous solution, the best device achieves a formate Faradaic efficiency of up to ~80%. Compared to a BPM-based MEA under similar conditions, our CEM-based MEA requires approximately 1.5 V lower voltage to sustain a current density of 300 mA cm^{-2}, demonstrating the effectiveness of our single-membrane configuration and surface functionalization strategy.

Among various formate-producing catalysts, bismuth-based materials stand out for their excellent selectivity and broad working potential window as previously demonstrated by our group and others.[26–29] Here, we selected nanostructured $Bi_2O_2CO_3$ as the precatalyst, which was prepared via a facile solvothermal method described in the Supporting Information. The powder X-ray diffraction (XRD) pattern of the product shows diffraction peaks characteristic of tetragonal $Bi_2O_2CO_3$ (Figure 2a). Scanning electron microscopy (SEM) image reveals that the product consists of nanosheets with a nearly square geometry, measuring approximately 200–800 nm in lateral dimensions and around 10 nm in thickness (Figure 2b,c). It is worth noting that under CO_2RR conditions, the $Bi_2O_2CO_3$ nanosheets are reduced to bismuth nanostructures, which function as the active catalyst for formate production.[28]

Electrochemical measurements were conducted by assembling $Bi_2O_2CO_3$-loaded GDE as the cathode, a Nafion membrane separator, and IrO_x-loaded Ti mesh as the anode in a 5 cm^2 MEA electrolyzer (see Experimental section for more details). The electrolyzer was continuously supplied with 1.5 M $KHCO_3$ as the catholyte at a flow rate of 50 mL min^{-1} and 0.5 M H_2SO_4 as the anolyte at 10 mL min^{-1}, unless otherwise specified. Importantly, the Nafion membrane enables the selective transport of protons from the anode to the cathode during the reaction, where they react with HCO_3^- in the catholyte to release CO_2 for CO_2RR. A dynamic equilibrium is established when the proton production rate from oxygen evolution reaction (OER) at the anode matches the proton consumption rate due to CO_2RR at the cathode.

Our investigations began with the unmodified catalyst under applied current densities ranging from 60 to 300 mA cm^{-2}. As shown in Figure 2d,e, the primary reduction product is H_2 from the competing hydrogen evolution reaction (HER), while formate is detected as a minor product, with its highest faradaic efficiency of 40% observed at a current density of 120 mA cm^{-2}. This result is expected, as the zero-gap configuration between the cathode and the Nafion membrane facilitates the conversion of bicarbonate to CO_2 but also leads to proton buildup at the cathode, which disfavors subsequent CO_2 reduction. This observation underscores the importance of carefully managing the electrode microenvironment during bicarbonate electrolysis, as both insufficient and excessive proton flux can compromise reaction selectivity.

To this end, we modified the catalyst surface with PiperION, a commercially available ionomer featuring high-density positive charges (Figure 2f). To improve the physical stability, the ionomer was added with 0.3 wt% of carbon black nanoparticles and then sprayed onto the working electrode surface to achieve an optimal thickness. Carbon black nanoparticles serve as a physical anchoring medium that immobilizes PiperION molecules through localized adsorption. SEM image shows that after the surface modification, the electrode surface is covered with a polymeric film blended with nanoparticles (Figure S1). Elemental mapping using X-ray energy dispersive spectroscopy (EDS) confirms the uniform distribution of nitrogen species from the piperidinium groups of PiperION (Figure 2g). This surface modification, with its high density of positive charges, is expected to repel protons and prevent their local accumulation at the cathode, thereby creating a partially alkaline microenvironment that is favorable to CO_2RR. As a result, the PiperION-modified catalyst demonstrates a reduced HER activity and significantly enhanced formate selectivity, achieving a maximum of 79.1% at 120 mA cm^{-2} and maintaining 38.1% even at 300 mA cm^{-2} (Figure 2h). Remarkably, only ~4.3 V is required to sustain a large current density of 300 mA cm^{-2} without the need for ohmic compensation. Additionally, this configuration largely suppresses formate crossover from the cathode to the anode (Figure S2).

We next investigated the effects of several experimental parameters for performance optimization. The layer thickness

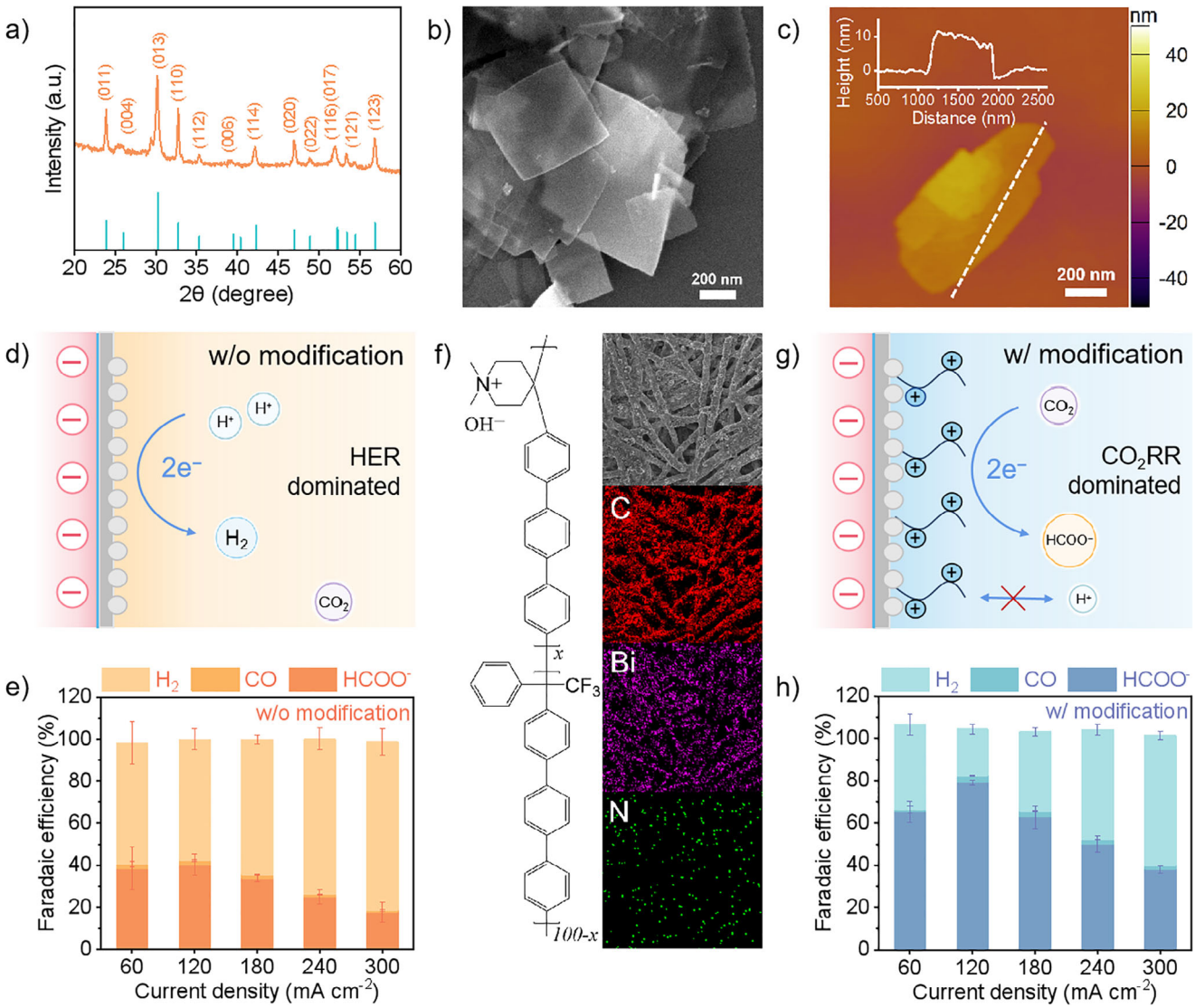

Figure 2. Structural characterizations of $Bi_2O_2CO_3$ nanosheets and significance of catalyst surface modification. a) XRD pattern, b) SEM image, c) AFM image with corresponding height profile of $Bi_2O_2CO_3$ nanosheets. d) Schematic illustrating the reaction on the unmodified catalyst surface. e) Product faradaic efficiencies on the unmodified catalyst surface under varying applied current densities. f) Chemical structure of PiperION and EDS mapping images of PiperION/C-modified catalyst surface. g) Schematic illustrating the reaction on the modified catalyst surface. h) Product faradaic efficiencies on the modified catalyst surface under varying applied current densities.

of the PiperION/C surface modification was first varied because it greatly impacts the electrode microenvironment by affecting its accessibility to the proton flux from the anode (Figures 3a and S3). The optimal surface loading of PiperION/C is found to be around 440 μg cm^{-2}, with the measured formate selectivity described above. Thinner (e.g., 220 μg cm^{-2}) or thicker (e.g., 880 μg cm^{-2}) surface modification layers both result in overall inferior performance. This observation can be justified by the fact that the former cannot effectively prevent proton surface buildup, while the latter would hinder CO_2 diffusion to the catalyst and increase the ionic impedance.

Ionomers with different chemical structures of cationic groups, positive charge densities, and ionic conductivities also play an important role when used for surface modification. We then compared several cationic ionomers at the same loading of 440 μg cm^{-2}, including Sustainion, Fumion FAA-3, and QAPPT, in addition to PiperION. Their chemical structures are detailed in the Supporting Information (Figure S4). All ionomer modifications successfully enhance the formate faradaic efficiency compared to the unmodified catalyst across current densities ranging from 60 to 300 mA cm^{-2} (Figures 3b and S5). Among them, PiperION is identified to be the most effective: at 120 mA cm^{-2}, the PiperION-modified catalyst exhibits about 20% greater formate selectivity compared to all other ionomer modifications. Even though the origin of its superiority currently remains elusive, we note that PiperION is advocated to have excellent ionic conductivity for bicarbonates,[30] and can facilitate their transport from the catholyte to the cathode-CEM interface, where they react with the incoming proton flux to release CO_2 for subsequent formate production.

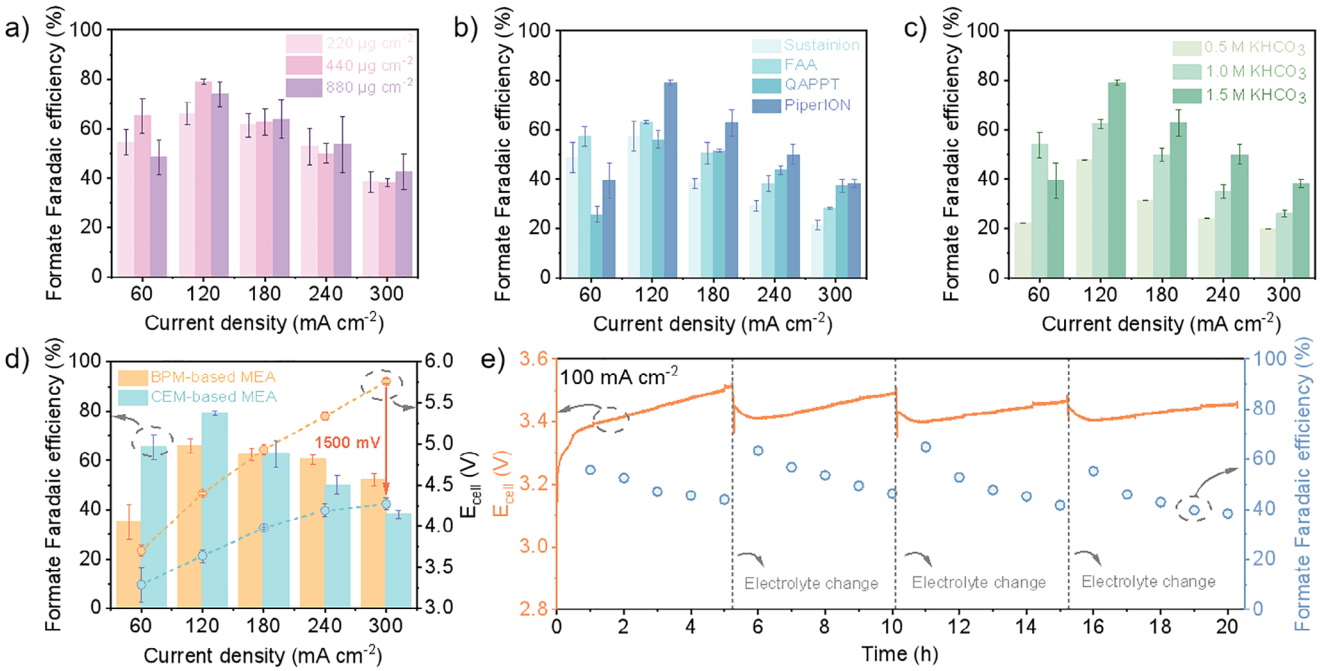

Figure 3. Bicarbonate electrolysis performance of the CEM-based MEA with the modified Bi catalyst. a)–c) Formate faradaic efficiencies with a) different PiperION/C loadings, b) different types of ionomers, and c) varying $KHCO_3$ concentrations. d) Comparison of formate faradaic efficiency and cell voltage between the BPM- and CEM-based MEA. e) Operation stability of the CEM-based MEA at 100 mA cm^{-2}, with dashed lines indicating when the electrolyte was replenished.

The bicarbonate concentration of the catholyte determines the potential CO_2 capacity that can be locally generated upon acidification and supplied to the catalyst and thus also affects the performance of bicarbonate electrolysis. Here, we varied the $KHCO_3$ concentration from 0.5 to 1.5 M under otherwise identical conditions. As illustrated in Figures 3c and S6, the formate faradaic efficiency greatly enhances as the concentration rises. At 120 mA cm^{-2}, the attainable selectivity is only 47% or 62% when 0.5 or 1.0 M $KHCO_3$ is in use, respectively. Further increasing the concentration beyond 1.5 M does not additionally benefit the selectivity. Furthermore, we investigated the effects of $KHCO_3$ flow rate and H_2SO_4 concentrations as summarized in Figure S7.

To highlight the advantages of our CEM-based MEA over BPM-based devices, we constructed a BPM-based MEA for comparison. This assembly included a similarly PiperION-modified cathode, a Fumasep FBM-PK BPM membrane separator, and NiFe-layered double hydroxide (LDH) grown on Ni foam as the anode (see Experimental section for more details). The anolyte was switched to 1 M KOH to capitalize on the excellent OER activity of NiFe LDH in alkaline solution.[31–33] Figure 3d compares the formate selectivity of both configurations. While the CEM-based MEA demonstrates significantly enhanced formate selectivity at lower current densities (<180 mA cm^{-2}), the BPM-based MEA exhibits higher selectivity at higher current densities. A notable contrast is seen in their operation voltages: the BPM-based MEA requires significantly higher working voltages than the CEM-based MEA. For example, the former requires 5.8 V to achieve a current density of 300 mA cm^{-2}, whereas only 4.3 V is needed for the same current density with the latter. Notably, our BPM-based MEA outperforms or matches similar devices reported in the literature.[24,25] The lower working voltage of the CEM-based MEA translates to higher energy efficiency, reflecting the unique advantage of the single-membrane configuration without sacrificing CO_2RR selectivity.

Furthermore, we evaluated the long-term operational stability of our CEM-based MEA with the PiperION-modified catalyst. During an initial 5 h electrolysis at 100 mA cm^{-2}, the working voltage gradually increases from 3.3 to 3.5 V, while the formate selectivity slightly decays from 56% to 44% (Figure 3e). This activity loss is attributed to the gradual depletion of bicarbonate in the catholyte over time, leading to a reduced local CO_2 supply and consequently lower CO_2RR selectivity. Replenishing the $KHCO_3$ electrolyte immediately restores the working voltage to 3.4 V and the formate selectivity to ~60% (Figure 3e). Such a reaction-replenish cycle can be periodically repeated for at least four consecutive cycles with a total of 20 h, evidencing no significant deterioration of the catalyst or its surface modification.

(Bi)carbonate electrolysis offers a viable solution to bridge the gap between CO_2 emissions and utilization. As the primary source of CO_2 emissions, flue gases typically contain 2%–15% of O_2 along with other impurities.[11,34] These gases, without prior purification, cannot be directly converted using gas-fed CO_2RR electrolyzers, as the presence of O_2 would dominate the cathodic reaction due to its more favorable reduction thermodynamics. To demonstrate this, we constructed a gas-fed anion-exchange membrane (AEM)-based MEA (Figure 4a) for CO_2RR to formate (see Experimental section for more details). When supplied

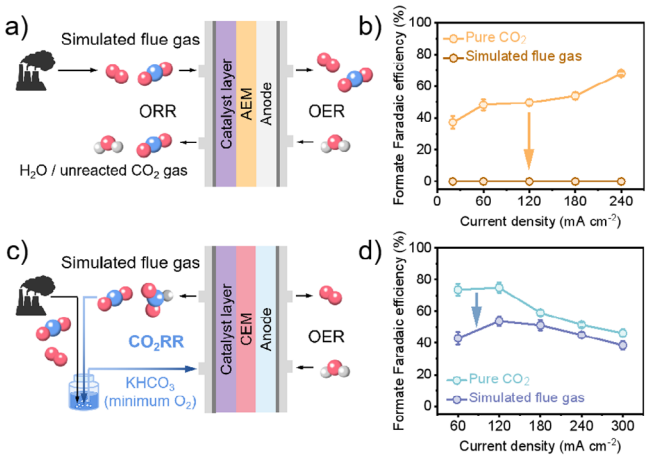

Figure 4. Conversion of simulated flue gas using the CEM-based MEA. a) Schematic illustrating the conversion of simulated flue gas using the gas-fed AEM-based MEA. b) Formate faradaic efficiency of the AEM-based MEA when fed with pure CO_2 or simulated flue gas. c) Schematic illustrating CO_2 capture from simulated flue gas and subsequent bicarbonate electrolysis using the capture solution from either pure CO_2 or simulated flue gas. d) Formate faradaic efficiency of the CEM-based MEA when fed with pure CO_2 or simulated flue gas.

with pure CO_2, the device exhibits a formate selectivity of 40%–70% (Figure 4b). The missing faradaic efficiency is attributed to formate crossover to the anode, where some of it undergoes oxidization (Figure S2).[35] However, when pure CO_2 is replaced with simulated flue gas (containing 15% of CO_2, 5% of O_2, and 80% N_2), CO_2RR is entirely suppressed, and no formate is detected at either the cathode or anode as expected (Figure 4b).

To enable bicarbonate electrolysis, the simulated flue gas was first bubbled into a KOH solution. This step converts dilute CO_2 in the flue gas into bicarbonate, which then is supplied to the CEM-based MEA for subsequent electrochemical reaction (Figure 4c). Even though O_2 has some solubility in water (1.2 mM at 1 atm and 298 K),[36] its concentration is significantly lower than the localized high concentration of CO_2 released from bicarbonate acidification and does not greatly interfere with CO_2RR despite its thermodynamic advantage. As a result, decent formate faradaic efficiency of 40%–50% is measured using the capture solution of flue gas as the catholyte, which is only slightly lower than the selectivity obtained with the capture solution of pure CO_2 for bicarbonate electrolysis (Figure 4d). Although there is still room for improvement, the results here showcase the promise of our CEM-based MEA for converting waste CO_2 to valuable products via bicarbonate electrolysis, offering potential alignment with flue gas point sources.

In summary, we reported a CEM-based MEA for efficient and O_2-tolerant bicarbonate electrolysis. By employing $Bi_2O_2CO_3$ nanosheets as the precatalyst, functionalized with the positively charged ionomer PiperION for microenvironment management, we achieved a significant enhancement in formate selectivity with a faradaic efficiency of up to 80% at high current densities. Our single-membrane CEM-based system outperformed conventional BPM-based MEAs in terms of voltage requirements for bicarbonate electrolysis. At 300 mA cm^{-2}, its full cell working voltage was about 1.5 V lower than that of the BPM-based system. Moreover, the system demonstrated resilience to O_2 impurities—a common challenge in flue gas CO_2 reduction—indicating that bicarbonate electrolysis could provide a practical solution for directly converting waste CO_2 without the need for O_2 removal or CO_2 purification steps. These findings highlight the potential of our CEM-based MEAs for scalable and efficient CO_2 conversion in industrial applications.

Acknowledgements

The authors acknowledge the support from the National Natural Science Foundation of China (52425209, 52161160331 and 22309126), Postdoctoral Fellowship Program of CPSF under Grant Number (GZC20231878), Jiangsu Funding Program for Excellent Postdoctoral Talent (2022ZB543), and the Collaborative Innovation Center of Suzhou Nano Science and Technology.

Conflict of Interests

The authors declare no conflict of interest.

Data Availability Statement

The data that support the findings of this study are available from the corresponding author upon reasonable request.

Keywords: Bicarbonate electrolysis · Cation exchange membrane · Membrane electrode assembly · Simulated flue gas · Surface modification

[1] P. De Luna, C. Hahn, D. Higgins, S. A. Jaffer, T. F. Jaramillo, E. H. Sargent, *Science* **2019**, *364*, eaav3506.
[2] O. S. Bushuyev, P. De Luna, C. T. Dinh, L. Tao, G. Saur, J. van de Lagemaat, S. O. Kelley, E. H. Sargent, *Joule* **2018**, *2*, 825–832.
[3] N. Han, P. Ding, L. He, Y. Li, Y. Li, *Adv. Energy Mater.* **2020**, *10*, 1902338.
[4] H. Shin, K. U. Hansen, F. Jiao, *Nat. Sustain.* **2021**, *4*, 911–919.
[5] M. G. Kibria, J. P. Edwards, C. M. Gabardo, C. T. Dinh, A. Seifitokaldani, D. Sinton, E. H. Sargent, *Adv. Mater.* **2019**, *31*, 1807166.
[6] Y. Luo, K. Zhang, Y. Li, Y. Wang, *InfoMat* **2021**, *3*, 1313–1332.
[7] E. W. Lees, B. A. Mowbray, F. G. Parlane, C. P. Berlinguette, *Nat. Rev. Mater.* **2022**, *7*, 55–64.
[8] X. She, Y. Wang, H. Xu, S. Chi Edman Tsang, S. Ping Lau, *Angew. Chem. Int. Ed.* **2022**, *61*, e202211396.
[9] M. Sassenburg, M. Kelly, S. Subramanian, W. A. Smith, T. Burdyny, *ACS Energy Lett.* **2023**, *8*, 321–331.
[10] J. A. Rabinowitz, M. W. Kanan, *Nat. Commun.* **2020**, *11*, 5231.
[11] N. J. Harmon, H. Wang, *Angew. Chem. Int. Ed.* **2022**, *61*, e202213782.
[12] K. Xing, J. Chen, Y. Li, *Natl. Sci. Open* **2024**, *3*, 20240039.
[13] I. Sullivan, A. Goryachev, I. A. Digdaya, X. Li, H. A. Atwater, D. A. Vermaas, C. Xiang, *Nat. Catal.* **2021**, *4*, 952–958.
[14] D. W. Keith, G. Holmes, D. S. Angelo, K. Heidel, *Joule* **2018**, *2*, 1573–1594.
[15] F. Zeman, *Environ. Sci. Technol.* **2007**, *41*, 7558–7563.

[16] G. Lee, Y. C. Li, J.-Y. Kim, T. Peng, D.-H. Nam, A. Sedighian Rasouli, F. Li, M. Luo, A. H. Ip, Y.-C. Joo, *Nat. Energy* **2021**, *6*, 46–53.
[17] B. M. Gallant, *Nat. Energy* **2021**, *6*, 13–14.
[18] H. Ma, E. Ibáñez-Alé, R. Ganganahalli, J. Pérez-Ramírez, N. López, B. S. Yeo, *J. Am. Chem. Soc.* **2023**, *145*, 24707–24716.
[19] K. Shen, D. Cheng, E. Reyes-Lopez, J. Jang, P. Sautet, C. G. Morales-Guio, *Joule* **2023**, *7*, 1260–1276.
[20] H. Liu, Y. Chen, J. Lee, S. Gu, W. Li, *ACS Energy Lett.* **2022**, *7*, 4483–4489.
[21] T. Li, E. W. Lees, M. Goldman, D. A. Salvatore, D. M. Weekes, C. P. Berlinguette, *Joule* **2019**, *3*, 1487–1497.
[22] G. Lee, A. S. Rasouli, B.-H. Lee, J. Zhang, Y. C. Xiao, J. P. Edwards, M. G. Lee, E. D. Jung, F. Arabyarmohammadi, H. Liu, *Joule* **2023**, *7*, 1277–1288.
[23] M. Shen, L. Ji, D. Cheng, Z. Wang, Q. Xue, S. Feng, Y. Luo, S. Chen, J. Wang, H. Zheng, *Joule* **2024**, *8*, 1999–2015.
[24] T. Li, E. W. Lees, Z. Zhang, C. P. Berlinguette, *ACS Energy Lett.* **2020**, *5*, 2624–2630.
[25] O. Gutiérrez-Sánchez, B. De Mot, M. Bulut, D. Pant, T. Breugelmans, *ACS Appl. Mater. Interfaces* **2022**, *14*, 30760–30771.
[26] N. Han, Y. Wang, H. Yang, J. Deng, J. Wu, Y. Li, Y. Li, *Nat. Commun.* **2018**, *9*, 1320.
[27] J. Fan, X. Zhao, X. Mao, J. Xu, N. Han, H. Yang, B. Pan, Y. Li, L. Wang, Y. Li, *Adv. Mater.* **2021**, *33*, 2100910.
[28] H. Yang, N. Han, J. Deng, J. Wu, Y. Wang, Y. Hu, P. Ding, Y. Li, Y. Li, J. Lu, *Adv. Energy Mater.* **2018**, *8*, 1801536.
[29] F. Yang, A. O. Elnabawy, R. Schimmenti, P. Song, J. Wang, Z. Peng, S. Yao, R. Deng, S. Song, Y. Lin, *Nat. Commun.* **2020**, *11*, 1088.
[30] B. Endrődi, E. Kecsenovity, A. Samu, T. Halmágyi, S. Rojas-Carbonell, L. Wang, Y. Yan, C. Janáky, *Energy Environ. Sci.* **2020**, *13*, 4098–4105.
[31] J. Wang, Z. Zhang, W. Wu, Y. Liu, B. Dong, Y. Wang, Y. Wang, *ACS Energy Lett.* **2024**, *9*, 110–117.
[32] Y. C. Li, D. Zhou, Z. Yan, R. H. Gonçalves, D. A. Salvatore, C. P. Berlinguette, T. E. Mallouk, *ACS Energy Lett.* **2016**, *1*, 1149–1153.
[33] D. A. Vermaas, W. A. Smith, *ACS Energy Lett.* **2016**, *1*, 1143–1148.
[34] U. Legrand, U.-P. Apfel, D. C. Boffito, J. R. Tavares, *J. CO2 Util.* **2020**, *42*, 101315.
[35] K. Peramaiah, M. Yi, I. Dutta, S. Chatterjee, H. Zhang, Z. Lai, K. W. Huang, *Adv. Mater.* **2024**, *36*, 2404980.
[36] W. Xing, G. Yin, J. Zhang, *Rotating Electrode Methods and Oxygen Reduction Electrocatalysts*, Elsevier, Amsterdam, **2014**, pp. 1–31.

Manuscript received: February 28, 2025
Revised manuscript received: May 02, 2025
Accepted manuscript online: May 12, 2025
Version of record online: ■■, ■■

Communication

CO_2 Reduction

K. Xing, M. Wang, B. Pan, C. Liang, Y. Li* — **e202504835**

Efficient Bicarbonate Electrolysis to Formate Enabled via Ionomer Surface Modification in Cation Exchange Membrane Electrolyzers

A new electrolyzer configuration, featuring a single cation exchange membrane and surface-modified bismuth catalyst, is designed for bicarbonate electrolysis. This configuration enables highly efficient production of formate and significantly reduced operating voltage, providing a potential solution for direct CO_2 utilization from point source emissions.